Light transmission through a subwavelength slit: Waveguiding and optical vortices

Hugo F. Schouten, Taco D. Visser,* and Daan Lenstra
Department of Physics and Astronomy, Free University, De Boelelaan 1081, 1081 HV Amsterdam, The Netherlands

Hans Blok
Department of Electrical Engineering, Delft University of Technology, Mekelweg 4, 2628 CD Delft, The Netherlands
(Received 19 December 2001; revised manuscript received 18 December 2002; published 14 March 2003)

The anomalous (i.e., more than 100%) light transmission through a subwavelength slit in a thin metal plate is accompanied by a combination of waveguiding and phase singularities of the field of power flow near the slit. The crucial role of these phase singularities (such as optical vortices and saddle points) in exciting the waveguide modes is systematically studied. We predict transmission efficiencies as high as 300% for certain configurations.

DOI: 10.1103/PhysRevE.67.036608 PACS number(s): 42.25.Bs, 42.25.Fx

The analysis of light transmission through a slit with a subwavelength width in a thin plate is a subject with a venerable history [1–3], dating back to Lord Rayleigh. Because of its importance for near-field optics and semiconductor technology, it continues to attract attention. Recently Ebbesen *et al.* observed extraordinary light transmission (i.e., more than 100%) through an array of subwavelength holes [4,5], which led to a new wave of interest in the subject. Broadly speaking there are two mechanisms involved in extraordinary light transmission: the coupling of light with surface plasmons [4–8], and Fabry-Pérot-like resonances inside the apertures [9–11].

In this paper we study the light transmission for a different configuration, namely, a single subwavelength slit in a metal plate of finite conductivity for the TE-polarization case (i.e., with the electric field parallel to the slit). TE polarization differs from TM polarization in that no surface plasmons are excited [12]. Furthermore, for TE polarization the first waveguide mode in a perfect conductor has a cutoff width of $w_{\text{cut-off}}=\lambda/2$, with λ being the wavelength. However, due to their finite conductivity, efficient energy transport may be possible at smaller slit widths in realistic metal plates. A rigorous computation of the field demonstrates that near these cutoff widths, there is an enhanced transmission through the slit. Transmission efficiencies as high as 300% are found for special configurations. We emphasize that these remarkable enhancement effects occur even though there is no coupling to surface plasmons.

To elucidate why the field couples so effectively with the propagating waveguide modes, we have analyzed the field of power flow (i.e., the time-averaged Poynting vector) near the slit. It is found that this field exhibits *optical vortices* and other kinds of *phase singularities* [13–15], which are arranged in an arraylike pattern. We find that the location and annihilation or creation of these phase singularities are intimately connected with the phenomenon of enhanced transmission.

*Electronic address: tvisser@nat.vu.nl;
URL: www.nat.vu.nl~tvisser

The field around a single, infinitely long, slit in a metal plate was calculated using a rigorous scattering approach [16]. The total electric field $\mathbf{E}$ is written as the sum of two parts, namely the incident field $\mathbf{E}^{(\text{inc})}$ and the scattered field $\mathbf{E}^{(\text{sca})}$. The incident field is the field that would occur in the absence of the slit in the plate. The illuminating field is taken to be monochromatic and propagating perpendicular to the plate. We have suppressed the time-dependent part of the field given by $\exp(-i\omega t)$, where ω denotes the angular frequency and $i=\sqrt{-1}$. The scattered field is the field due to the presence of the slit. By converting Maxwell's equations into an integral equation, we obtain the expression [16]

$$\mathbf{E}=\mathbf{E}^{(\text{inc})}-i\omega\Delta\varepsilon\int_{\text{slit}}\overleftrightarrow{\mathbf{G}}\mathbf{E}\,d^2r, \tag{1}$$

where $\Delta\varepsilon=\varepsilon_0-\varepsilon_{\text{plate}}$ is the difference in permittivity of the slit (vacuum) and the plate, and $\overleftrightarrow{\mathbf{G}}$ is the electric Green's tensor pertaining to the plate without the slit. For points within the slit, Eq. (1) is a Fredholm equation of the second kind for $\mathbf{E}$, which was solved numerically by the collocation method with piecewise-constant basis functions [17]. The transmission coefficient of the slit, T, is defined as the difference of the normal (i.e., z) components of the actual time-averaged Poynting vector $\langle\mathbf{S}\rangle$ and that of the Poynting vector in the absence of the slit $\langle\mathbf{S}^{\text{inc}}\rangle$ integrated over the dark side of the plate. This is normalized by the integral of the normal component of $\langle\mathbf{S}^{(0)}\rangle$, the Poynting vector of the field emitted by the source and impinging on the slit, i.e.,

$$T\equiv\frac{\displaystyle\int_{\text{slit}}\langle S_z\rangle_{z=d}\,d^2x+\int_{\text{plate}}(\langle S_z\rangle-\langle S_z^{(\text{inc})}\rangle)_{z=d}\,d^2x}{\displaystyle\int_{\text{slit}}\langle S_z^{(0)}\rangle_{z=0}\,d^2x}, \tag{2}$$

where d is the thickness of the metal plate. It is to be noted that the second integral in the numerator extends over the entire plate. This is because a small part of the transmitted field may flow through the plate rather than through the slit. In practice, the integrand tends to zero in a distance of about a wavelength from the slit. The term $\langle S_z^{(\text{inc})}\rangle$ is typically negligible for metal plates, but not, e.g., for thin semiconductor plates.

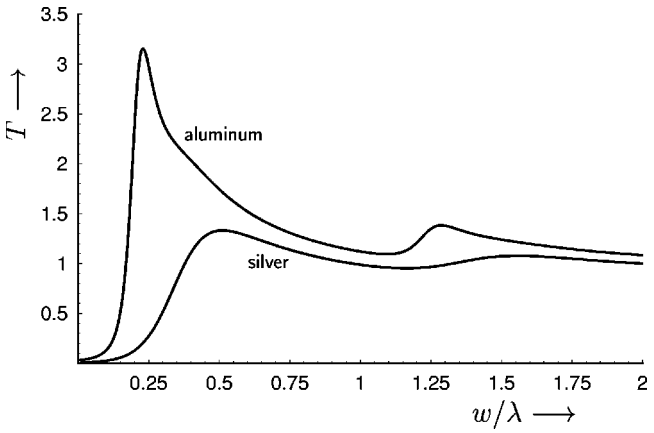

FIG. 1. The transmission coefficient T of a narrow slit in a thin plate as a function of the slit width w, expressed in wavelengths. The lower curve is for a slit in a 100-nm-thick silver plate and $\lambda = 500$ nm. The upper curve is for a slit in a 100-nm-thick aluminum plate and $\lambda = 91.8$ nm. At these wavelengths the refractive indices are taken as $n_{\text{silver}} = 0.05 + i2.87$ and $n_{\text{aluminum}} = 0.041 + i0.517$, respectively.

In Fig. 1 (lower curve) the transmission coefficient is shown as a function of the width of a slit in a thin silver plate. The upper curve is discussed later. We observe a damped resonance behavior as a function of the width w, with maxima at $w \approx 0.5\lambda, 1.5\lambda, \ldots$, where the transmission is enhanced, i.e., the transmission coefficient is greater than one, with its largest value $T = 1.33$ at $w = 0.5\lambda$.

If the dispersion relation is computed for the first guided mode [18] of a silver waveguide, it is found that, due to the finite conductivity, the cutoff width is less than that for a perfectly conducting metal, viz., $w_{\text{cut-off}} = 0.4\lambda$ (see Fig. 2). The position of the maxima in the transmission as a function of the slit width is found to be close to the cutoff width; see

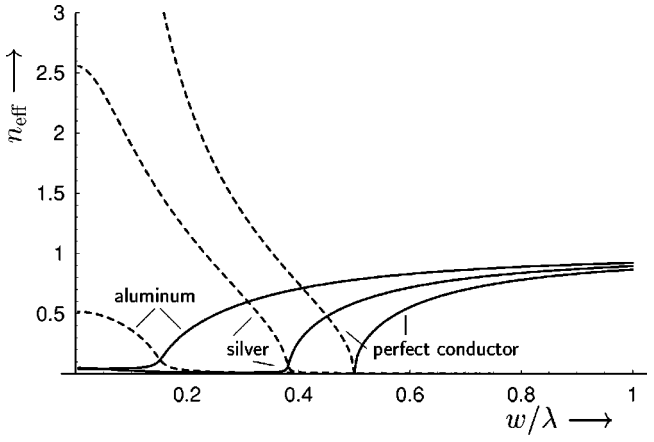

FIG. 2. Effective indices n_{eff} of the first waveguide mode inside a narrow slit as a function of the slit width w, expressed in wavelengths. The full lines denote the real part of the effective index, the dashed lines denote the imaginary part. The two curves for aluminum are for $\lambda = 91.8$ nm, the two curves for silver are for $\lambda = 500$ nm, whereas the last two curves are for a perfectly conducting material. The refractive indices were taken to be $n_{\text{silver}} = 0.05 + i2.87$ and $n_{\text{aluminum}} = 0.041 + i0.517$.

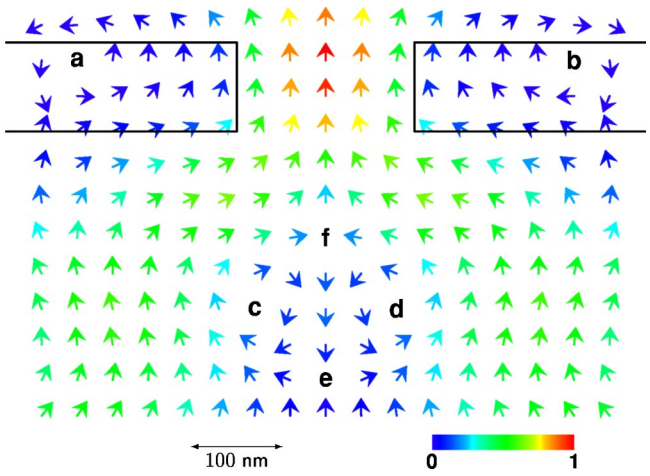

FIG. 3. Behavior of the time-averaged Poynting vector near a 200-nm wide slit in a 100-nm-thick silver plate. The incident light (coming from below) has a wavelength $\lambda = 500$ nm. The left-handed (a and d) and right-handed (b and c) optical vortices each have a topological charge of $+1$, whereas the topological charge of the saddle points (e and f) is -1. The transmission coefficient $T = 1.11$. The color coding indicates the modulus of the (normalized) Poynting vector (see legend).

Figs. 1 and 2. This also holds for the higher-order modes.

If the conductivity of the metal decreases, the cutoff width shifts to lower values. This is illustrated in Fig. 2 (left-hand curves), where the effective index is plotted for aluminum at $\lambda = 91.8$ nm. It is seen that the cutoff width is shifted to $w \approx 0.15\lambda$. Because the normalization factor of the transmission coefficient [Eq. (2)] will be smaller for smaller values of the width, it is to be expected that the anomalous transmission will be greater for materials with a smaller cutoff width. In Fig. 1 the transmission coefficient for a slit in aluminum is shown. Both the expected shift of the maximum to a lower value is observed, as well as the enhancement in the transmission, with a maximum of $T \approx 3.2$ at $w \approx 0.25\lambda$.

To understand this anomalous transmission, we have analyzed the field of power flow near the slit. A typical example of these calculations is shown in Fig. 3 (for the thin silver plate, discussed before), where the field is seen to exhibit phase singularities, i.e., points where the amplitude of the time-averaged Poynting vector is zero and as a consequence its direction, or equivalently its phase, is undetermined. It is seen that the anomalous transmission (namely, $T = 1.11$) coincides with the presence of two optical vortices (a and b) *within* the plate, and a funnellike power flow into the slit. This funnellike effect corresponds to a transmission coefficient of more than one. In addition, four other phase singularities are visible just below the slit (c, d, e, and f; two saddle points and two vortices). In Fig. 4 the location of the phase singularities is shown on a larger scale. It is seen that they are arranged in an arraylike pattern. It is to be noted that only part of the phase singularities are shown—the pattern is continuous in a periodic way to the left and right, and also downwards.

Changing the slit width in a continuous manner causes the phase singularities to move through space. Near the cutoff

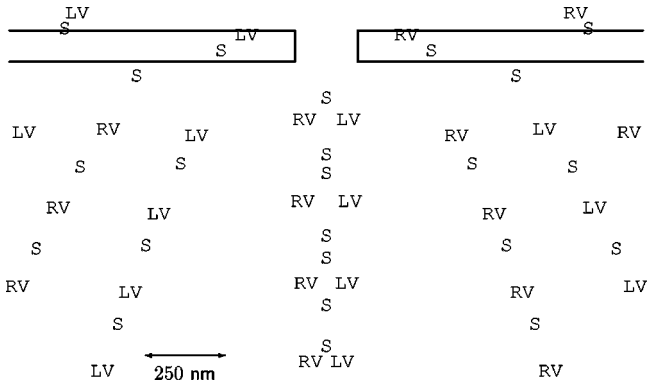

FIG. 4. Location of phase singularities in the field of power flow for the same configuration as in Fig. 3, i.e., for a slit width of $w=0.4\lambda=200$ nm. The left- and right-handed optical vortices are denoted by LV and RV, respectively; S denotes a saddle point. Notice the larger scale as compared to Fig. 3.

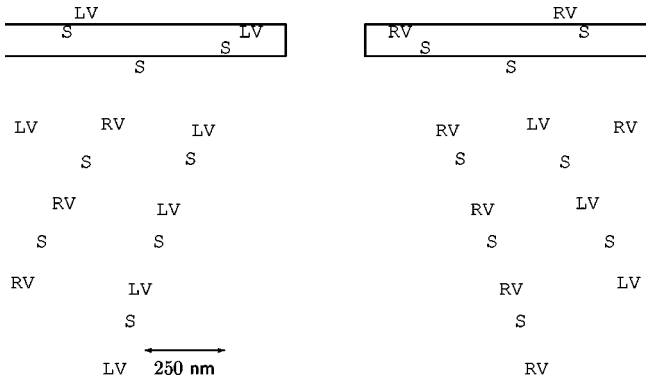

FIG. 5. Location of phase singularities in the field of power flow for the same configuration as in Fig. 4, but now for a slit width $w=0.5\lambda=250$ nm. Notice that the central array of phase singularities which was visible below the slit in Fig. 4 has now been annihilated.

width (at $w\approx0.45\lambda$) the array of phase singularities along the symmetry axis annihilate, each annihilation consisting of two vortices (one left handed and one right handed) and two saddle points. In Fig. 5 the resulting arrangement for $w=0.5\lambda$ is shown. Because the annihilation of phase singularities leads to a smoother field of power flow, an increased transmission is observed. Near the other cutoff widths at $w\approx1.4\lambda, 2.4\lambda, \ldots$ additional annihilations occur. In such processes the total topological charge is always conserved [19,20].

If the field of power flow is analyzed for a slit in an aluminum plate (at $\lambda=91.8$ nm), the same pattern and behavior of the phase singularities as a function of the slit width is found as described above. Below the cutoff width, the same pattern of phase singularities is found as in Figs. 3 and 4. At a width slightly higher than the cutoff width (i.e., at $w=0.2\lambda$) an array of phase singularities along the symmetry axis annihilates. Again, at the cutoff widths of the higher modes similar annihilations occur. The described behavior of the pattern of phase singularities was also found for other materials with $\mathrm{Re}(n)\ll\mathrm{Im}(n)$ (i.e., good conductors, below a plasma resonance frequency).

In conclusion, we have shown that anomalous light transmission through a narrow slit in a thin metal plate is described by both waveguiding and phase singularities of the field of power flow. The onset of guided modes yields the maxima of the transmission curve, while a qualitative understanding of the light transmission is obtained by charting the different phase singularities in the field of power flow. In particular, it was found for certain configurations that transmission efficiencies as high as three are possible. We notice that in this particular configuration no plasmons are excited.

Because of the ability of subwavelength slits to ''focus'' a large amount of the power flow onto a small area, our findings are relevant for the design of different subwavelength light sources. These could be used in near-field optics, optical recording, and lithography to obtain subwavelength resolution.

This research was supported by the Dutch Technology Foundation STW and the European Union, within the framework of the Future and Emerging Technologies program (SLAM). The authors wish to thank Dr. G. Gbur for stimulating discussions.

[1] Lord Rayleigh, Philos. Mag. **43**, 259 (1897); reprinted in *The Scientific Papers of Lord Rayleigh* (Dover, New York, 1964).
[2] C.J. Bouwkamp, Rep. Prog. Phys. **17**, 35 (1954).
[3] M. Born and E. Wolf, *Principles of Optics*, 7th ed. (Cambridge University Press, Cambridge, 1999), Sec. 11.8.3.
[4] T.W. Ebbesen *et al.*, Nature (London) **391**, 667 (1998).
[5] H.F. Ghaemi *et al.*, Phys. Rev. B **58**, 6779 (1998).
[6] U. Schröter and D. Heitmann, Phys. Rev. B **58**, 15 419 (1998).
[7] J.A. Porto, F.J. García-Vidal, and J.B. Pendry, Phys. Rev. Lett. **83**, 2845 (1999).
[8] L. Martín-Moreno *et al.*, Phys. Rev. Lett. **86**, 1114 (2001).
[9] S. Astilean, Ph. Lalanne, and M. Palamaru, Opt. Commun. **175**, 265 (2000).
[10] Y. Takakura, Phys. Rev. Lett. **86**, 5601 (2001).
[11] F. Yang and J.R. Sambles, Phys. Rev. Lett. **89**, 063901 (2002).
[12] H. Raether, *Surface Plasmons on Smooth and Rough Surfaces and on Gratings* (Springer, Berlin, 1988).
[13] J.F. Nye and M.V. Berry, Proc. R. Soc. London, Ser. A **336**, 165 (1974).
[14] M.V. Berry, in *Physics of Defects*, edited by R. Balian, M. Kléman, and J.-P. Poirier (North-Holland, Amsterdam, 1981), p. 453.
[15] J.F. Nye, *Natural Focusing and Fine Structure of Light* (IOP, Bristol, 1999).
[16] T.D. Visser, H. Blok, and D. Lenstra, Int. J. Quantum Chem. **35**, 240 (1999).
[17] K.E. Atkinson, *A Survey of Numerical Methods of Fredholm*

Equations of the Second Kind (SIAM, Philidelphia, 1976), Chap. 2.

[18] A.W. Snyder and J.D. Love, *Optical Waveguide Theory* (Chapman and Hall, London, 1983), Chap. 12.

[19] A. Boivin, J. Dow, and E. Wolf, J. Opt. Soc. Am. **57**, 1171 (1967).

[20] G.P. Karman, M.W. Beijersbergen, A. van Duijl, and J.P. Woerdman, Opt. Lett. **22**, 1503 (1997).